The shapes and sizes of two domains of tropomodulin, the P-end-capping protein of actin-tropomyosin

Tetsuro Fujisawa*, Alla Kostyukova[1], Yuichiro Maéda

Laboratory for Structural Biochemistry, RIKEN Harima Institute at SPring-8, 1-1-1 Kouto, Mikazuki, Sayo, Hyogo 679-5148, Japan

Received 10 October 2000; revised 2 May 2001; accepted 8 May 2001

First published online 17 May 2001

Edited by Amy M. McGough

Abstract Tropomodulin, the P-end (slow-growing end)-capping protein of the actin-tropomyosin filament, and its fragment (C20) of the C-terminal half were studied by synchrotron small-angle X-ray scattering, restoring low-resolution shapes using an ab initio shape-determining procedure. Tropomodulin is elongated (115 Å long) and consists of two domains, one of 65 Å in length and the other being similar to C20 in shape and size if the long axes of the two are tilted by about 40° relative to each other. We propose a model for tropomodulin in association with tropomyosin and actin: the N-terminal half of tropomodulin, a rod, binds to the N-terminus of tropomyosin and the C-terminal triangle domain protrudes from the P-end being slightly bent towards the actin subunit at the end, thereby blocking the P-end. © 2001 Published by Elsevier Science B.V. on behalf of the Federation of European Biochemical Societies.

Key words: Actin-capping protein; Tropomyosin-binding protein; Muscle thin filament; Actin dynamics; Small-angle X-ray scattering

1. Introduction

Tropomodulin is the unique P-end (slow-growing end)-capping protein of the actin-tropomyosin filament. It was originally found [1] as a tropomyosin-binding protein in the short actin filament located at the junction of the spectrin network lining the erythrocyte membrane. In muscle, tropomodulin is localized at the P-end of the thin filament. Tropomodulin blocks the elongation and depolymerization of actin, thereby regulating the length of the actin-tropomyosin filament. While tropomodulin maintains constant thin filament lengths, it allows monomer exchange at the same time. It has also been suggested that tropomodulin's capping activity is regulated by conformations and/or strain of the thin filament [2]. Although the functions of this protein have been well documented, little is known about its structure. Knowledge of its detailed 3D structure is essential for understanding the capping mechanism. As the first step for protein crystallographic study of this protein, we have established an improved *Escherichia coli*-based expression system for tropomodulin [3]. Using this system, large fragments have been obtained; Tmod(N39)is a nearly complete molecule, C20 is a fragment of the C-terminal half, N11 is a fragment that covers one quarter (N11) of the N-terminus. Limited proteolysis and spectroscopic analyses of these species have revealed that tropomodulin is an α-helix-rich protein and that each half of the molecule has a distinct property; the N-terminal half is likely to be extended or to form a highly flexible structure, whereas the C-terminal half is compactly folded [3]. We have also confirmed that the binding site(s) for tropomyosin exists in the N-terminal region of tropomodulin, as was previously reported [4,5]. It is known that tropomodulin binds to the N-terminus of tropomyosin. In the present study, from the small-angle X-ray scattering (SAXS) patterns, the shape and size of the whole molecule and C20 of tropomodulin have been deduced by use of an ab initio fitting procedure. Based on the low-resolution structure, we propose a model for the actin-tropomyosin–tropomodulin complex.

2. Materials and methods

2.1. Tropomodulin preparation

Tmod (N39) (amino acids 1–344, lacking 15 amino acids at the C-terminus and with a histidine tag, Met-His_6, at the N-terminus) of chicken E-tropomodulin origin (for isoforms of tropomodulin, see [6]) was overexpressed in *E. coli* and purified, and C-terminal half C20 (amino acids 160–344) was prepared by proteolysis of Tmod (N39) with *Staphylococcus aureus* V8 protease as described previously [3]. After purification, protein solutions were dialyzed against the buffer solution used for X-ray measurements (20 mM Tris–HCl, pH 7.6, 1 mM DTT) and concentrated using Centricon-10 to a final concentration of 4.6 mg ml^{-1} for Tmod (N39) or 4 mg ml^{-1} for C20. Protein concentration was determined by using a micro protein determination kit (Sigma) with bovine serum albumin as the standard. Samples were checked by SDS– and native PAGE before and after measurements. On the gels, both Tmod (N39) and C20 formed single bands, indicating that the preparations used were of high purity and that no substantial degradation nor aggregation had occurred during the measurements.

2.2. SAXS and data treatment

SAXS measurements were carried out using RIKEN structural biology beamline I (BL45XU) [7], which accepts X-ray at wave length of 1.0 Å from an undulator source of the electron storage ring SPring-8. With a detector consisting of an X-ray image intensifier and cooled CCD (XR-II+CCD) [8], each scattering profile was collected at 20°C for 1 s. The sample-to-detector distance was 60 or 220 cm. Judging from the stability of intensity vs. time, there was no radiation damage of protein preparations during data collection. Preliminary data processing was performed using the program *iisgnapr* [9]. The reciprocal parameter, S, which is equal to $2\sin\theta/\lambda$ (where 2θ is the scattering angle and λ is the X-ray wavelength), was calibrated by the meridional reflections from chicken collagen. The radius of gyration, R_g, was determined by fitting the intensity profiles using Guinier approximation: $I(S) = I(0)\exp(-4\pi^2 R_g^2 S^2/3)$, where $I(0)$ is the forward scattering intensity at a zero angle [10], with fitting ranges of S^2 ($Å^{-2}$) from 5×10^{-6} to 30×10^{-6} and from 25×10^{-6} to 100×10^{-6} for

*Corresponding author. Fax: (81)-791-58 2836.
E-mail: fujisawa@spring8.or.jp

[1] Present address: Institute of Protein Research RAS, Pushchino, Moscow Region 1142290, Russia.

0014-5793/01/$20.00 © 2001 Published by Elsevier Science B.V. on behalf of the Federation of European Biochemical Societies.
PII: S0014-5793(01)02498-X

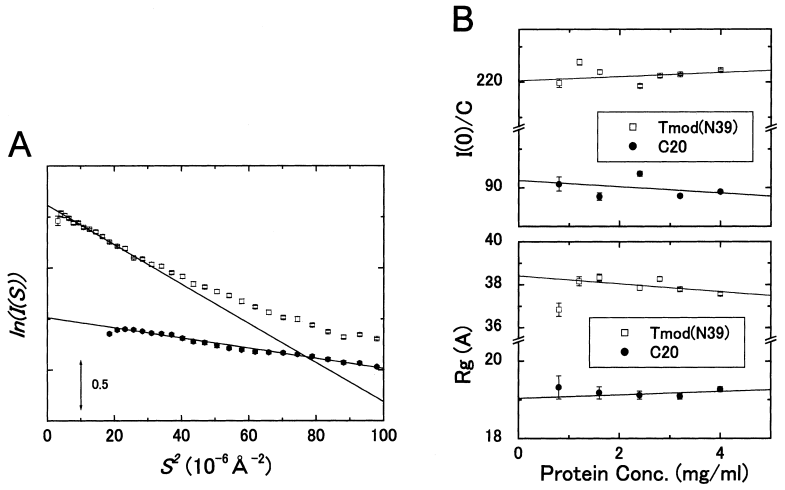

Fig. 1. A: Guinier plots of X-ray scattering intensity from Tmod (N39) (open squares) and C20 (filled circles). The ordinate is in an arbitrary unit, and for clarity, two sets of data points have been shifted relative to each other along the ordinate axis. The *S*/*N* ratio is so good that the error bars of each point were invisible. B: Protein concentration dependency on R_g and $I(0)/C$. The symbols are the same as those in A. If aggregates exists, both $I(0)/C$ and R_g increase with increasing protein concentration C (mg ml^{-1}).

Tmod (N39) and C20, respectively. In order to eliminate inter-particle interference, measurements were repeated at five or seven different protein concentrations, from 0.8 to 5.9 mg ml^{-1}, and these data points were extrapolated to zero protein concentration. The cross-sectional radius of gyration, R_c, was determined by fitting the data points using the equation $I(S)S = I_c(0)\exp(-p^2R_c^2S^2/2)$ over ranges S^2 (Å^{-2}) from 50×10^{-6} to 200×10^{-6} and from 100×10^{-6} to 450×10^{-6} for Tmod (N39) and C20, respectively (data not shown). The pair distance distribution functions were evaluated by the indirect transform package *GNOM* [11,12] and XCALC [13]. The procedure of determination of D_{max} is described elsewhere [14].

2.3. Low-resolution shape determination of tropomodulin structures

Low-resolution particle shapes were restored from the scattering intensity profiles using two fitting procedures: a classical fitting to a cylinder and an ab initio procedure of DAMMIN [15]. In the dummy atom minimization (DAMMIN), a protein molecule is approximated by densely packed small spheres (dummy atoms). Minimization was performed using the simulated annealing method [15], starting from the dummy atoms placed at random coordinates within the search sphere, sphere of diameter D_{max}. The configuration X of dummy atoms were optimized so as to minimize $f(X) = \chi^2 + \alpha P(X)$, where $P(X)$ is the looseness penalty function to avoid rough surface and α is a weighing factor that increases as χ^2 decreases. In the former method, the intensity function was fitted to a cylindrical scattering function:

$$I(S) = \int_0^1 \frac{4J_1^2(2\pi SR)}{(2\pi SR)^2}\frac{\sin^2(\pi HxS)}{(\pi HxS)^2}\mathrm{d}x$$

where R and H are radius and height of a cylinder, respectively. J_1 is a Bessel function of first order. Fitting was conducted with the intensity profile within the range of S from 0 to $2N_S$, where $N_S = D_{max}S_{max}$, D_{max} is the maximum dimension of a particle (obtainable as the zero crossing point of $P(r)$) and S_{max} is the largest recorded S. This is based on the theory proposed by Shannon and Weaver (see [13]) that n sectors (Shannon channels each having a width of N_S wide each) contain information equivalent to specifying n parameters in a fitting.

The stability of the model was checked by repeating the minimization more than 10 times, each being from different initial coordinates. The deviations among models were quantified by calculating three ellipsoidal axes for each model using the *XLATTICE* program [16]. The difference in the three axial ratios between these models should be normally within a few percent. 3D models are displayed using the program VMD [17]. For Tmod (N39), initially the search sphere (diameter, 115 Å) contained 1505 dummy atoms with a radius of 4.5 Å. In the final model, 194 dummy atoms were attributed to the particle. For C20, initially 1686 dummy atoms with a radius of 2.25 Å were placed in the search sphere (diameter, 60 Å), being reduced to 585 dummy atoms in the final model. For both cases, about 3 500 000 models were evaluated and final 60–80 models are in the similar level of *R*-factors.

3. Results

3.1. Radius of gyration and maximal dimension of tropomodulin molecules

The Guinier plots of the scattering intensity profiles indicate no upward curvature (Fig. 1A) and $I(0)$ was constant with increasing protein concentration (Fig. 1B). The zero extrapolation $I(0)$ of the profiles is consistent with the molecular weights, indicating that no aggregates had formed in either preparation measured. Thus, $I(0) = 91$ (an arbitrary unit) was obtained from C20 and $I(0) = 222$ was obtained from N39, whereas $I(0) = 73$ was obtained from myoglobin (MW = 17.1 kDa, at 3 mg ml^{-1}) on the same beamline at the same time, giving rise to MW = 21.5 kDa for C20 and 52.0 kDa for N39,

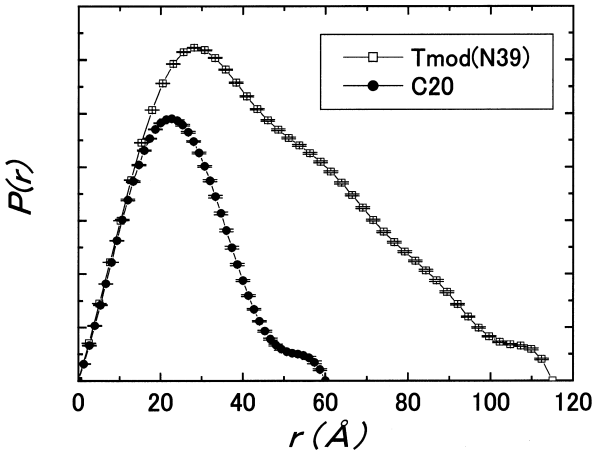

Fig. 2. The pair distance distribution functions $P(r)$ for Tmod(N39) (solid line) and C20 (dotted line). The ranges of $I(S)$ used for $P(r)$ calculation were 0.002 Å^{-1} to 0.04 Å^{-1} for Tmod (N39) and 0.005 Å^{-1} to 0.04 Å^{-1} for C20.

Table 1
Summary of structural parameters determined by SAXS

Molecules	Values obtained directly from Guinier plot and cross-sectional plot scattering intensity data				Parameters for cylindrical fit	
	R_g (Å)	$I(0)$	D_{max} (Å)	R_c (Å)	Radius (Å)	Height (Å)
Tmod (N39)	38.09 ± 0.29	222.4 ± 1.2	115 ± 5	11.92 ± 0.026	18.9	129
C20	18.96 ± 0.23	91.2 ± 0.4	62.5 ± 2.5	11.15 ± 0.027	15.8	53.8

The error of D_{max} was estimated from the procedure described elsewhere [14].

respectively. These MW estimations are compatible with real data. The radius of gyration R_g and D_{max} were obtained from the Guinier plot (Fig. 1A) and from the pair distribution function $P(r)$ (Fig. 2), respectively, and these values are summarized in Table 1. The data indicate that Tmod (N39) is an elongated protein, because the molecule has an extraordinary large R_g for a protein of this weight (39 kDa) and because the profile of $P(r)$ is typical for an elongated particle. C20 (MW = 20.6 kDa) must be more globular, since R_g was determined to be 19 Å, which is close to that of a globular protein of similar weight, myoglobin (R_g = 17.7 Å, MW = 17.1 kDa), although it is still rather elongated as the profile of $P(r)$ indicates.

3.2. Shape of tropomodulin

Each scattering intensity profile was first fitted by a solid cylinder that is specified by two parameters, height (H) and radius (R), as summarized in Table 1. Although the fitting was conducted using the portion of the intensity profile up to $N_S = 2$ (sufficient for determining two parameters), fitting was rather good beyond this region of S. This indicates that both Tmod (N39) and C20 are approximately cylindrical in shape (Fig. 3). In the case of $S > 0.02$ Å^{-1}, the cylindrical fitting deviates from the scattering data: As the resolution increases, the particle cannot be approximated by a simple solid cylinder. The resemblance to a cylindrical shape in low resolution is also supported by the fact that the radii of gyration of a cross-sectional area R_c, which are obtained directly from the profile (Table 1), and the radii of the cylindrical fitting R's are consistent with R_c's with the relation of $R = \sqrt{2} \times R_c$. Second, in order to deduce the shapes of tropomodulin, an ab initio fitting procedure, DAMMIN, was used, and the restored envelopes together with the fits to the experimental data are shown in Fig. 3. The χ^2 values of model fitting to experimental data in the range of 0.0023 Å^{-1} < S < 0.0398 Å^{-1} were 29.77 and 915.76 for DAMMIN and cylinder fitting, respectively.

The uniqueness of the restored envelopes was ensured as

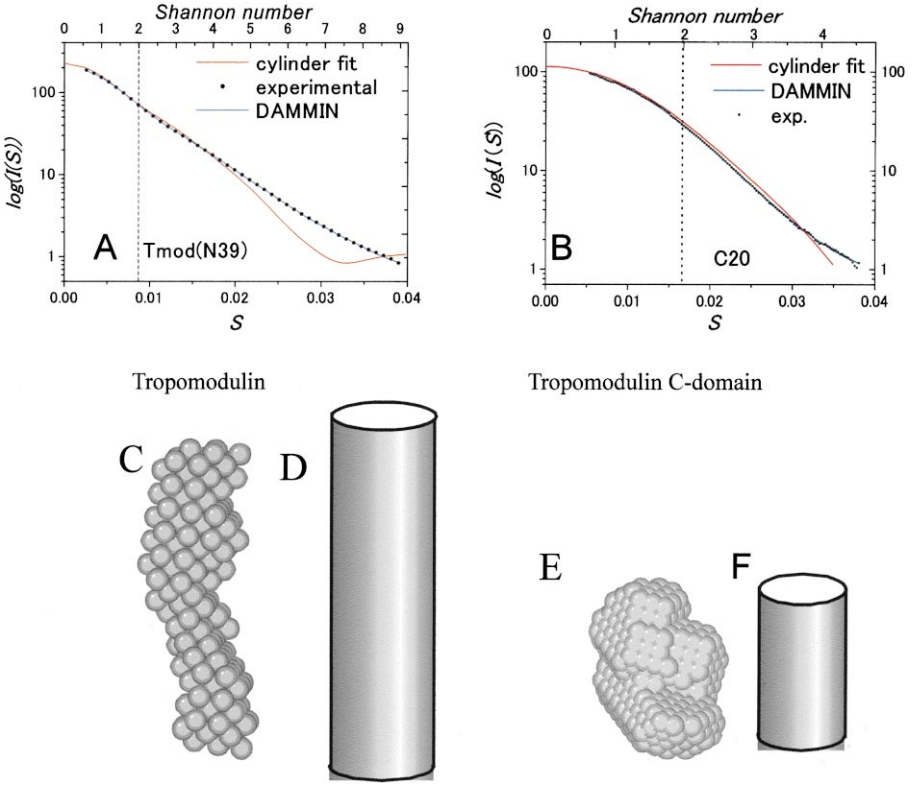

Fig. 3. Comparison of the scattering intensity data with fitted curves. Tmod (N39) (A) and for C20 (B). In each graph, the scattering intensity is indicated as a dotted curve, while the best fit by a solid cylinder is indicated as a solid curve in red and the best fit by DAMMIN fitting is indicated as a solid curve in blue. Here again, the error bars of experimental data are invisible in this size of plots. The models used for the best fits either by the cylindrical fitting (D and F) or by the DAMMIN fitting (C and E) are shown in the lower panel. C and D are for Tmod (N39), while E and F are for C20.

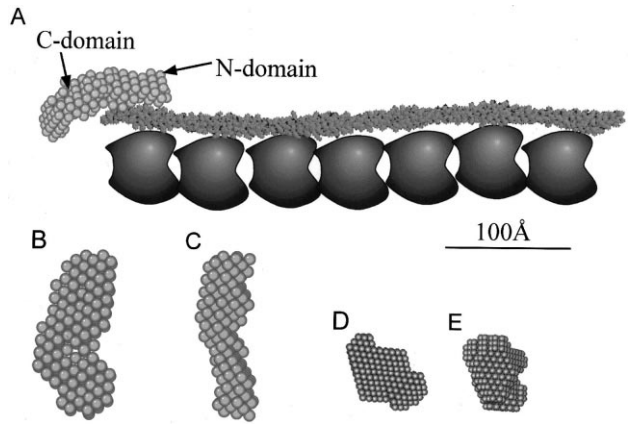

Fig. 4. A: Proposed model for the complex of actin-tropomyosin–tropomodulin. Depicted are actin subunits with one tropomyosin at the P-end of one strand only. A tropomodulin molecule is represented as the one obtained by the DAMMIN fitting (Fig. 3). The helical arrangement of the molecules is totally neglected in this schematic representation. The atomic coordinates of tropomyosin are those according to the model of Dr. Haruki Nakamura (Osaka University) [23]. B–E: Models obtained by the DAMMIN fitting. B and C are for Tmod (N39), while D and E are for C20. B: (D) is a front view, whereas C (E) is a side view; the two viewing directions are related by a rotation of 90° around the long axis of Tmod (N39), which is vertical. The long axis of C20 is rotated by 40° relative to the long axis of Tmod (N39), which brings about the best superposition of C20 to the lower half of Tmod (N39).

follows. First, independent runs of the fitting yielded envelopes that are similar to each other. For Tmod (N39), S.D./mean is 8.1% for the axial ratio x/z or 7.1% for y/z ($n=9$). For C20, the value is 4.4% for x/z or 4.4% for y/z ($n=10$). Second, the restored envelopes by DAMMIN resemble simple cylinders which fit the experimental intensity profiles beyond $N_S=2$ (Fig. 3). Third, the envelope of the globular portion of Tmod (N39) correlates well with the envelope of C20, even though the two envelopes have been obtained independently. Moreover, the volume ratio Tmod (N39) to C20 was estimated to be 2.65 by DAMMIN fitting, which is consistent with the $I(0)$ ratio (about 2.43 in Table 1).

4. Discussion

The present study has demonstrated the solution structures of Tmod(N39) and C20 with different levels of SAXS analyses, showing the validity of the DAMMIN fitting procedure. Since many more parameters than the number of Shannon channels N_S, are determined by the DAMMIN procedure, the uniqueness of the solution is always in discussion. If the procedure is valid, the models analyzed by different levels of SAXS analyses should coincide with each other within the limits of individual resolutions. We previously employed classical solid body modeling rather than spherical harmonics expansion [14]. This is because, for an elongated molecule, spherical harmonics expansion needs higher harmonics and the truncation error is therefore large, which hampers good fitting.

The present study has indicated that Tmod (N39) is an elongated molecule of 115 Å in length, being consistent with the hydrodynamic properties of tropomodulin [1]. The envelope of Tmod (N39) indicates that the molecule consists of two domains with dimensions of 40 Å × 60 Å × 20–30 Å and 50 Å × 50 Å × 20–30 Å, respectively. The latter domain is slightly bent (by about 40°) relative to the axis of the first domain. The latter domain has a similar shape to that C20, which is like a rotary ellipsoid of 54 Å in length and 35 Å in thickness C20 can be superposed well on the flat triangle of Tmod (N39) if the long axes of the two are tilted by about 40° relative to each other. We conclude therefore that the first domain is assigned mostly to the N-terminal half, whereas the latter is assigned to the C-terminal half of the molecule.

Based on the shape and size of tropomodulin as described above, we herewith propose a model for the complex of actin-tropomyosin–tropomodulin (Fig. 4). The elongated N-terminal half of tropomodulin interacts with the N-terminal region of tropomyosin, so that this portion is placed along with tropomyosin. The C-terminal half, a flat triangle domain, must protrude from the P-end of the actin-tropomyosin filament, as originally implied by electron micrographs of rotary shadowed particles of tropomodulin with tropomyosin [18]. Since the tropomodulin molecule is slightly bent at the junction between N- and C-terminal halves, the protruded part might be slightly bent towards the filament axis. Moreover, there might be two tropomodulin molecules per P-end, one being associated with each of the two tropomyosin strands (see [19]). Therefore, a pair of tropomodulin molecules may inhibit depolymerization and elongation of the actin filament even without direct interaction of tropomodulin with actin. At present, details of the tropomodulin-actin interaction are not known. It has been shown that tropomodulin alone, without tropomyosin, decreases the rates of polymerization and depolymerization at the P-end of F-actin [20]. Recent study has indicated that this inhibitory role of tropomodulin is played by the C-terminal half, but not the N-terminal half of the molecule. This implies that there might be direct interaction, despite weak and non-specific, between tropomodulin and actin [21]. Regardless of whether or not tropomodulin interacts directly with actin, the P-end of the actin-tropomyosin filament is likely to have an extension of about 60 Å in length, consisting of the C-terminal halves of tropomodulin. This is consistent with a previous observation that the striated muscle thin filament end distal to the Z-line is extended by about 55 Å (a unit length of the actin molecule) beyond the end of the last tropomyosin molecule [22].

Finally, the model indicated in Fig. 4 clearly shows what question should be addressed next. Tropomodulin interacts with tropomyosin and actin. Each pair of interactions is contributed by each half of the tropomodulin molecule. Details of the site and the manner of interactions should be elucidated. Also of crucial importance is to understand possible cross-talks between two pairs of interactions through the connection between the two domains.

Acknowledgements: We are grateful to Dr. Yukihiro Nishikawa for the fine graphical figures and to Dr. Haruki Nakamura of Osaka University for the coordinates of his 3D model for tropomyosin. This work was supported in part by the Special Coordination Funds of the Ministry of Education, Culture, Sports, Science and Technology, the Japanese Government.

References

[1] Fowler, V.M. (1987) J. Biol. Chem. 262, 12792–12800.
[2] Littlefield, R. and Fowler, V.M. (1998) Annu. Rev. Cell Dev. Biol. 14, 487–525.

[3] Kostyukova, A., Maeda, K., Yamauchi, E., Krieger, I. and Maéda, Y. (2000) Eur. J. Biochem. 267, 1–6.
[4] Babcock, G.G. and Fowler, V.M. (1994) J. Biol. Chem. 269, 27510–27518.
[5] Vera, C., Sood, A., Gao, K.M., Yee, L.J., Lin, J.J. and Sung, L.A. (2000) Arch. Biochem. Biophys. 378, 16–24.
[6] Almenar-Queralt, A., Lee, A., Conley, C.A., Ribas de Pouplana, L. and Fowler, V.M. (1999) J. Biol. Chem. 274, 28466–28475.
[7] Fujisawa, T. et al. (2000) J. Appl. Crystallogr. 33, 797–800.
[8] Amemiya, Y., Ito, K., Yagi, N., Asano, Y., Wakabayashi, K., Ueki, T. and Endo, T. (1995) Rev. Sci. Instrum. 66, 2290–2294.
[9] Fujisawa, T., Inoko, Y. and Yagi, N. (1999) J. Synchrotron Rad. 6, 1106–1114.
[10] Guinier, A. and Fournet, G. (1955), Wiley, New York.
[11] Svergun, D.I., Semenyuk, A.V. and Feigin, L.A. (1988) Acta Crystallogr. A 44, 244–250.
[12] Svergun, D.I. (1993) J. Appl. Crystallogr. 26, 258–267.
[13] Moore, P.B. (1980) J. Appl. Crystallogr. 13, 168–175.
[14] Fujisawa, T., Uruga, T., Yamaizumi, Z., Inoko, Y., Nishimura, S. and Ueki, T. (1994) J. Biochem. 115, 875–880.
[15] Svergun, D.I. (1999) Biophys. J. 76, 2879–2886.
[16] Walther, D., Cohen, F.E. and Doniach, S. (2000) J. Appl. Crystallogr. 33, 350–363.
[17] Humphrey, W., Dalke, A. and Schulten, K. (1996) J. Mol. Graph. 14.1, 33–38.
[18] Fowler, V.M. (1990) J. Cell. Biol. 111, 471–481.
[19] Fowler, V.M., Sussmann, M.A., Miller, P.G., Flucher, B.E. and Daniels, M.P. (1993) J. Cell. Biol. 120, 411–420.
[20] Weber, A., Pennise, C.R., Babcock, G.G. and Fowler, V.M. (1994) J. Cell. Biol. 127, 1627–1635.
[21] Fowler, V., Moyer, J., Almenar-Queralt, A. and Fritz-Six, K. (2001) Mol. Biol. Cell 11 (Suppl.), 557a.
[22] Ohtsuki, I. (1975) J. Biochem. Tokyo 77, 633–639.
[23] Nakamura, H. (1996) Q. Rev. Biophys. 29, 1–90.